Available online at www.sciencedirect.com
SCIENCE DIRECT®
Journal of Nuclear Materials 342 (2005) 1–7
journal of nuclear materials
www.elsevier.com/locate/jnucmat

Dynamics of high-temperature oxidation accompanied by scale removal and implications for technological applications

Jinsuo Zhang [a,*], Ning Li [b], Yitung Chen [c]

[a] Nuclear Design and Risk Analysis (D-5), Ms-K575, Decision Application Division, Los Alamos National Laboratory, Los Alamos, NM 87545, USA
[b] Materials Science and Technology Division, Los Alamos National Laboratory, Los Alamos, NM 87545, USA
[c] Mechanical Engineering Department, University of Nevada, Las Vegas, NV 89154, USA

Received 24 August 2004; accepted 19 January 2005

Abstract

The dynamics of a broad class of high-temperature oxidation accompanied by scale dissociation, volatilization, corrosion and erosion is theoretically analyzed through a dimensionless Tedmon's equation. The dependence of early stage, transition and asymptotic dynamics on oxidation (parabolic) and scale removal (linear) rate constants, and oxide initial conditions, are classified into distinct and universal categories. This analysis provides a simple yet powerful roadmap to study material performance in many technologically important applications, including the use of early stage measurement to predict long-term behaviors and screen materials.

1. Introduction

High-temperature oxidation of metals is of great scientific and technological importance. It plays an important role in the selection of materials for constructions or industrial equipments. If the oxides are protective, and the environment is stabilizing, then purposefully growing and maintaining oxides can be used to prevent or reduce corrosion by other mechanisms.

Scale removal affects many high-temperature oxidation processes with important technological applications. It can proceed through scale dissociation, volatilization, corrosion, erosion, etc. In high-temperature oxidation applications where corrosion exists, scale removal thins the protective layer and may lead to higher corrosion. On the other hand, scale removal can be applied to control the oxide layer thickness. It has been recognized that very thick oxide layer becomes structurally unstable and may break away.

High-temperature oxidation with scale removal has broad applications in the design of materials for fossil, solar, nuclear power reactors, passivation and oxidation of semiconductors, oxidation of materials developed and tested for fusion and fission energy systems. As such it has been widely studied for different purposes [1–11]. Recently, it is being intensively studied for corrosion mitigation in liquid lead–alloys (liquid lead, lead–bismuth eutectic) cooled advanced reactors and accelerator-driven systems [12].

Liquid lead–alloys appear to be the best coolant for advance nuclear reactors. For reducing the corrosion

* Corresponding author. Tel.: +1 505 667 7444; fax: +1 505 665 2897.
E-mail address: jzhang@cnls.lanl.gov (J. Zhang).

0022-3115/$ - see front matter © 2005 Elsevier B.V. All rights reserved.
doi:10.1016/j.jnucmat.2005.03.003

rate and forming the protective oxide layer, the oxygen concentration in the liquid is controlled in a reasonable range [12]. The structure materials (Fe–Cr alloy) are therefore subjected to both oxidation and mass transfer corrosion. The present study is mainly motivated by studying the protective oxide layer behavior in liquid lead–alloy systems, while the information in this study is generic for any environment containing linear scale removal and parabolic oxidation.

Generally, high-temperature oxidation with scale removal simultaneously involves both thermodynamics and kinetics. Because of the fast oxidation reaction, the process reaches local thermodynamic equilibrium quickly. Kinetics, such as species diffusion, becomes the most important and dominates. In the temperature range of interest, the kinetics can be described by a parabolic rate constant for oxidation, K_p, and a linear rate constant for scale removal, K_r [3]. The oxide thickness, x, observes Tedmon's equation [1]:

$$\frac{dx}{dt} = \frac{K_p}{2x} - K_r. \tag{1}$$

The solution for $x(t = 0) = 0$ (no pre-oxidation) is

$$t = -\frac{x}{K_r} - \frac{K_p}{2K_r^2} \ln\left|1 - \frac{2K_r}{K_p}x\right|. \tag{2}$$

Tedmon's original model for high-temperature oxidation with scale removal has been verified in several experiments. However, this form of the solution (Eq. 2) does not lend itself for conveniently analyzing kinetics, and no expression for mass change can be derived simply from Eq. (2).

In the present study, Tedmon's model is normalized for a universal description of oxidation with scale removal. The initial and asymptotic (long-term) kinetics are discussed and simple expressions for the kinetics are presented. The model is extended to include pre-oxidation cases. The dependence of early stage, transition and asymptotic dynamics on oxidation (parabolic) and scale removal (linear) rate constants, and oxide initial conditions, are classified into distinct categories. The weight change is analyzed using the non-dimensional variables. The present analysis provides a simple yet powerful roadmap to study material performance in many technologically important applications, including the use of early stage measurement to predict long-term behaviors and screen materials.

2. Modification of Tedmon's original model

Noting that Eq. (1) is demarcated by $x < x_f$ for oxide growth and $x > x_f$ for oxide thinning, where

$$x_f = \frac{K_p}{2K_r}. \tag{3}$$

It is clear that x_f is the asymptotic oxide thickness, assuming it is structurally stable (no spalling). The oxide thickness and time can then be scaled as

$$X = \frac{x}{x_f} = \frac{2K_r x}{K_p}, \quad \tau = \frac{t}{t_c} = \frac{2K_r^2 t}{K_p}, \tag{4}$$

where $t_c = K_p/2K_r^2 = x_f/K_r$ is not the time for achieving the asymptotic thickness. It is twice the time needed to reach the asymptotic oxide thickness following a pure parabolic growth law. Eq. (2) becomes:

$$\tau = -X - \ln|1 - X|. \tag{5}$$

When $X \to 1$ or $\tau \to \infty$, Eq. (5) can be approximated as

$$X(\tau \to \infty) = 1 - \exp(-\tau - 1), \tag{6}$$

which illustrates that the asymptotic kinetics as exponential approach. For early stages, the approximate solution becomes [2]:

$$X(\tau \to 0) = (2\tau)^{1/2} - \frac{2}{3}\tau. \tag{7}$$

The first term in the right side of Eq. (7) is the parabolic law, while the second term represents two-third of the linear scale removal. So the initial parabolic growth is reduced by the linear removal with the apparent removal rate reduced by 1/3. Such solution explicitly shows that the initial kinetics and the interaction of the two processes (oxide growth and scale removal) at early stages.

Comparisons between the initial and asymptotic kinetics with the exact solution are shown in Fig. 1, as well as the parabolic law. While the parabolic law over-predicts significantly even at $\tau = 0.0637$, $X = 0.3158$ by 13%, the second order approximation (Eq. (7)) only under-predicts by 2% at $\tau = 0.257$, $X = 0.5569$.

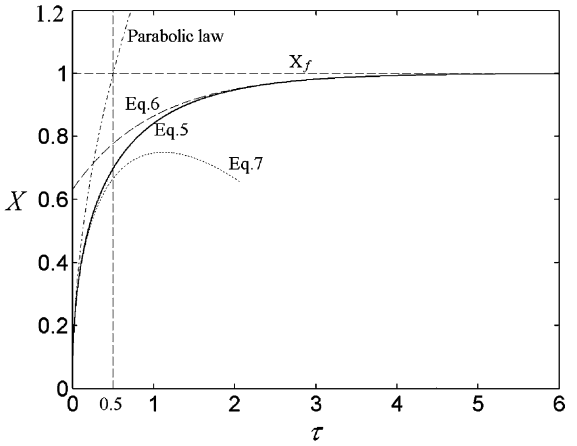

Fig. 1. Initial (Eq. (7)) and asymptotic kinetics (Eq. (6)) compared with the exact solution (Eq. (5)). The parabolic law is also shown.

The figure indicates that it is reasonable to analyze long-term behaviors based on short-term experiments. Eq. (7) can be applied to analyze the short-term experiments and provides the rate constants that can be substitute into Eq. (6) to predict the long-term behaviors. The figure also shows that there is a transition period in which neither Eq. (6) nor Eq. (7) is valid.

3. Extending Tedmon's original model to include pre-oxidation

Pre-oxidation can be an effective method to establish a protective oxide layer. For pre-oxidized materials, the initial condition of the Tedmon's model becomes:

$$X = X_0 \quad \text{at} \quad \tau = 0, \tag{8}$$

where X_0 is the non-dimensional pre-oxidation thickness. The solution of Eq. (1) is

$$\tau = -(X - X_0) - \ln\left|\frac{1-X}{1-X_0}\right|. \tag{9}$$

Clearly, $X_f = 1$ is the asymptotic oxide thickness. Based on Eq. (9), the asymptotic kinetics can be expressed as

$$X(\tau \to \infty) = 1 - (1 - X_0)\exp(-\tau - 1 + X_0). \tag{10}$$

If $X_0 = 0$, the solution is reduced to the original Tedmon's model.

Case I: $0 < X_0 < 1$.

This corresponds to $dX/d\tau > 0$, or thickening of the oxide. X approaches 1 from below.

For $0 < X_0 \ll 1$. Eq. (7) can be applied to analyze the initial kinetics by shifting the time origin back by $\tau_0 = -X_0 - \ln(1 - X_0)$. Then:

$$X(\tau \to 0) = (2\tau + 2\tau_0)^{1/2} - \frac{2}{3}(\tau + \tau_0). \tag{11}$$

For $0 \ll X_0 < 1$, the initial oxide growth can be approximately calculated using a second order approximation based on Eq. (1):

$$X(\tau \to 0) = X_0 + \left(\frac{1}{X_0} - 1\right)\tau - \frac{1}{2}\left(\frac{1}{X_0^3} - \frac{1}{X_0^2}\right)\tau^2. \tag{12}$$

The changes of the non-dimensional thickness in time are shown in Fig. 2 for $X_0 = 0.1$ and $X_0 = 0.8$, with the approximation results. The thickness approaches the limit similarly to that in the case of $X_0 = 0$ (Fig. 1). The asymptotic kinetics can be expressed by Eq. (10) for any X_0 in the range of (0, 1).

Case II: $X_0 = 1$.

This corresponds to $dX/d\tau = 0$, or constant oxide thickness. No new oxide forms on the surface and all the metal ions diffusing through the existing oxide scale are removed by the flowing liquid.

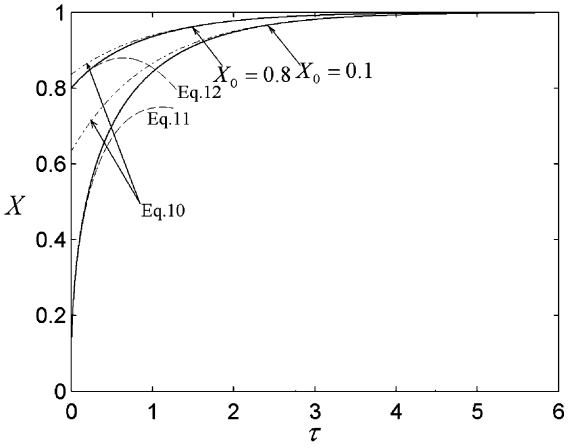

Fig. 2. Variations of the oxide thickness in time for $X_0 = 0.1$ and $X_0 = 0.8$. The dashed lines are from the approximations of the initial and asymptotic kinetics.

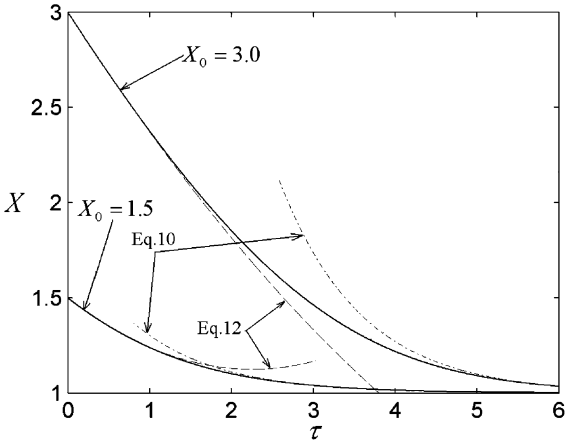

Fig. 3. Variations of the oxide thickness in time for $X_0 = 1.5$ and $X_0 = 3$. The dashed lines are from the approximations of the initial and asymptotic kinetics.

Case III: $X_0 > 1$.

This corresponds to $dX/d\tau < 0$, or thinning of the oxide. X approaches 1 from above. For this case, the initial and asymptotic kinetics can be approximated using Eqs. (12) and (10) respectively. The changes of oxide thickness in time for $X_0 = 1.5$ and $X_0 = 3.0$, as well as the initial and asymptotic approximations, are shown in Fig. 3.

4. Domains for approximations of initial and asymptotic kinetics

To apply the approximation expressions for the early states and long-term operations, their valid ranges

should be determined. The domains for valid approximations of initial and asymptotic kinetics can be shown in maps of τ and pre-oxidation thickness X_0. With 3% allowable deviation, the maps are shown in Fig. 4 for $0 \leqslant X_0 < 1$ and $X_0 > 1$.

For $0 \leqslant X_0 < 1$, Fig. 4(a) indicates that the valid range of the asymptotic approximation (Eq. (10)) increases with increasing pre-oxidation thickness. For $X_0 > 0.85$, the approximation can be applied to the entire time domain within 3% deviation. The parabolic law modified by linear scale removal (Eq. (11)) becomes invalid when the pre-oxidation thickness exceeds about 0.63. The valid range of the second order approximation for the early stages (Eq. (12)) also increases with increasing pre-oxidation thickness. Fig. 4(a) also indicates that there is a gap in which neither approximation for the early stage nor the asymptotic solution is valid. This is categorized as the transition period in the present study.

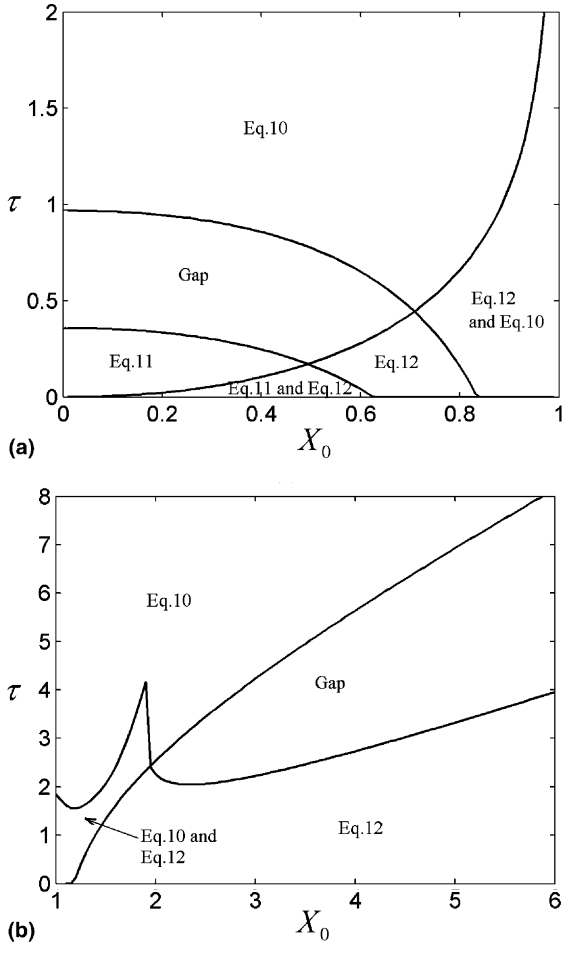

Fig. 4. Domains for approximations of the initial and asymptotic kinetics: (a) $0 \leqslant X_0 < 1$; (b) $X_0 > 1$.

For $X_0 > 1$, Fig. 4(b) shows that the valid domain for the asymptotic kinetics becomes larger when the pre-oxidation thickness approaches 1. When $X_0 < 1.2$, the asymptotic kinetics approximation can be applied to the entire time domain. The valid range of the second order approximation increases with increasing pre-oxidation thickness. There is also a transition period similar to that in the case of $0 \leqslant X_0 < 1$.

These two maps, Fig. 4(a) and (b), illustrate several key points. First, they determine the time intervals for the early stage kinetics and the asymptotic kinetics, and what approximation should be used in a specific time interval. Second, it is possible to analyze short-term experimental results and predict long-term behaviors using the asymptotic kinetics expression and to reduce the reliance on long-term experiments. Third, when the oxide thickness is near the limit, the evolution follows an exponential law (Eq. (10)).

5. Weight change analysis

Compared with measuring the oxide thickness, it is sometimes easier to measure the weight changes that can be derived from the proceeding discussions. For a sample with pre-oxidation thickness X_0, the weight change includes two parts: weight gain through oxidation that can be expressed as: $\rho_{ox} f_O x_f (X - X_0)$; and weight loss through corrosion that is $\rho_{ox}(1 - f_O) K_r t$. Therefore the specific weight change per unit area can be expressed as

$$\Delta w = \rho_{ox} f_O x_f (X - X_0) - \rho_{ox}(1 - f_O) K_r t, \tag{13}$$

where ρ_{ox} is the oxide density, and f_O is the mass fraction of oxygen in the oxide. If the weight change per unit area is non-dimensionalized as: $\Delta W = \Delta w / \rho_{ox} x_f$, Eq. (13) becomes:

$$\Delta W = f_O (X - X_0) - (1 - f_O)\tau. \tag{14}$$

The weight change rate $R_{\Delta W}$ is

$$R_{\Delta W} = \frac{d\Delta W}{d\tau} = f_O \frac{dX}{d\tau} - (1 - f_O). \tag{15}$$

Clearly for $X \to 1$ and $\tau \to \infty$, $R_{\Delta W} = -(1 - f_O)$, indicating that the asymptotic weight change has a linear loss rate.

When $X_0 = 0$ (no pre-oxidation), the weight change reaches a peak ΔW_p:

$$\Delta W_p = f_O^2 + (1 - f_O)[f_O + \ln(1 - f_O)], \tag{16}$$

at

$$\tau_p = -f_O - \ln(1 - f_O) \quad \text{and} \quad X_p = f_O. \tag{17}$$

Therefore, for $\tau < \tau_p$, $R_{\Delta W} > 0$, corresponding to weight gain (oxidation dominates in the early stage); for $\tau > \tau_p$, $R_{\Delta W} < 0$, corresponding to weight loss (scale removal dominates over the long run).

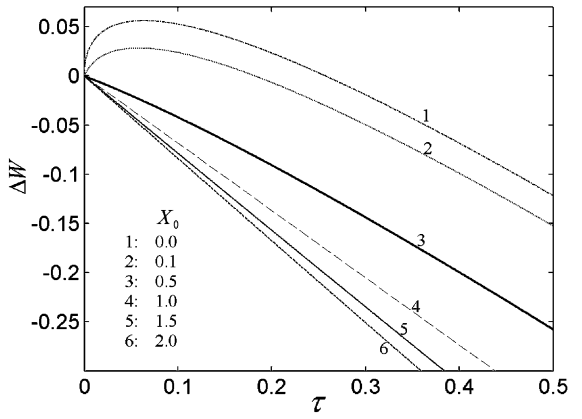

Fig. 5. Weight changes in time for different pre-oxidation thickness for $f_O = 0.3158$ (Fe_3O_4). The time for reaching the weight gain peak for $X_0 < f_O$ is much smaller than that for approaching the asymptotic oxide thickness. All asymptotic weight loss rates are the same $(1 - f_O)$.

When $X_0 < f_O$, the weight change peak becomes:

$$\Delta W_p = f_O(f_O - X_0) + (1 - f_O)\left[f_O + X_0 + \ln\left(\frac{1 - f_O}{1 - X_0}\right)\right]. \tag{18}$$

The initial weight gain still exists.

When $X_0 \geqslant f_O$, X_p is already exceeded, and $R_{\Delta W} < 0$, corresponding to weight loss for the entire duration. The weight changes for different pre-oxidation thicknesses are shown in Fig. 5.

For weight change at the early stage, Eqs. (11) and (12) for oxide thickness can be employed, therefore:

$$\Delta W = -f_O X_0 + f_O(2\tau + 2\tau_0)^{1/2} - \left(1 - \frac{1}{3}f_O\right)\tau - \frac{2}{3}f_O\tau_0 \tag{19a}$$

for $0 \leqslant X_0 < 1$, and

$$\Delta W = -\left(1 - \frac{f_O}{X_0}\right)\tau - \frac{1}{2}f_O\left(\frac{1}{X_0^3} - \frac{1}{X_0^2}\right)\tau^2 \tag{19b}$$

for $0 \leqslant X_0 < 1$ and $X_0 > 1$. Eqs. (19a) and (19b) can be easily applied to fitting the weight change measurement data from short-term experiments and calculating the rate constants K_p and K_r.

6. Technological implications and discussions

Motivated by the studies of protective oxide layer behaviors in liquid lead–alloy coolant system, Tedmon's original model for Cr oxidation with volatilization is extended to high-temperature oxidation with parabolic law and linear scale removal for any initial pre-oxidation condition. The scale removal may result from scale dissociation, volatilization, corrosion and erosion, etc. The initial conditions are classified into distinct categories. For deriving expressions of the weight changes, the early stage and asymptotic approximations of the oxide thickness are discussed. Simple expressions for analyzing the experimental results are obtained. The analysis gives a clear and simple roadmap to investigate specific materials and conditions of scientific and technological importance.

For measurement and analysis of oxidation with scale removal, this study shows how the oxide thickness and weight change data can be used, what simplified model is applicable in what range with what initial conditions.

For applications utilizing passivation or oxidation to protect substrate materials, this study provides a complete set of quantitative selection criteria for materials and operating conditions. Because of the influence of scale removal and the scale thickness limit imposed by structural stability, there are conclusions that appear paradoxical until now. The discovery will lead to re-thinking of some conventional wisdom.

The discussion for applications is best conducted with the inclusion of the physical parameters, i.e. K_p and K_r in this case. First, the asymptotic thickness $x_f = K_p/2K_r$ has to be structurally stable for the entire process to proceed as discussed, otherwise the scale may spall and the oxidation process will reset and start from the beginning. Since initial oxidation is rapid and lead to accelerated wastage of the substrate materials, this is undesirable. This constraint leads to the following criterion:

$$x_f = K_p/2K_r < x_s, \tag{20}$$

where x_s is the limit for structurally stable oxide scale. It is usually tens of microns or less.

Typically materials of high oxidation resistance are among the first to be selected, and the oxygen partial pressure of the environment is minimized. However, if K_r is reduced even more than the reduction in K_p, the oxide may grow too thick, spall off, and re-grow at the much faster initial rate. The overall long-term corrosion of materials could be worse than in conditions where K_r is higher for complying with the criterion (Eq. (20)). In the case of using active oxygen control to reduce corrosion of steels in heavy liquid metal coolant (lead–bismuth or lead), this leads to the need of keeping oxygen concentrations which is limited by criterion (Eq. (20)) at the highest temperature and oxygen saturation at the lowest temperature in closed circulation systems.

Under the condition that $x_f < x_s$, the long-term material thinning rate, R_r, is

$$R_r = \frac{\rho_{ox}}{\rho_M}(1 - f_O)K_r, \tag{21}$$

where ρ_M is the metal density. The above equation indicates that it is the scale removal rate that determines the steady state recession rate of the substrate. Knowing the design limit for the maximal wastage allowance, the lifetime estimate can be derived through Eq. (21).

Using pre-oxidation to enhance protection still requires the maintenance of oxygen activity in order to keep the oxide stable. Otherwise the oxide will be gradually removed. With the oxygen partial pressure or concentration set to a constant value, it is possible to vary the linear scale removal rate to make the oxide thickness satisfy Eq. (20). For example, this can be achieved by varying the liquid flow velocity in the mass transfer corrosion case, such as liquid metal coolant system subjected to corrosion.

It is also possible to pre-oxide materials in a condition that favors one oxidation mechanism and oxide over the others, and results in better protection in the early stage and even over the long run in practical applications with different achievable conditions. For instance, steels with relatively high Cr may be pre-oxidized at intermediate temperature and low oxygen partial pressure, and later used in high-temperature applications. The pre-oxidation condition favors the formation of non-porous tenacious Cr_2O_3, which may lead to a later process dominated by Cr oxidation and scale removal, as opposed to in situ formation of Cr–Fe spinel and Fe_3O_4 (magnetite) layers at higher operating temperatures that is dominated by Fe oxidation and scale removal. The detailed analysis of these scenarios will be reported in another paper.

In the present study, oxide thickness and time are normalized by x_f and t_c, respectively. Both of them are very sensitive to K_r, especially the time scale t_c. A very large t_c indicates that it takes a long time to approach the asymptotic oxide thickness. For a specified pre-oxidation thickness X_0, the oxide variation depends on the value of K_r. If K_r is small so that $X_0 < x_f$, the oxide thickness increases in time and approaches x_f from below; if K_r is large so that $X_0 > x_f$, the oxide thickness decreases in time and approaches x_f from above.

If the linear removal rate constant is sufficiently small so that $x_f > x_s$, then x_f cannot be achieved because spallation may occur when the oxide thickness reaches x_s. For such cases, the present model for predicting the final oxide thickness needs to be expanded, while it is expected that the new oxide layer formation at the spallation is still following the present law. Such situations should be avoided in engineering applications where oxidation is needed for protective purposes, therefore we focuses on the materials without oxide spallation in the short term. The present analysis is based on the assumption of parabolic oxidation. However, it is easy to be extended to the others such as the cubic law. Such extension for cases without pre-oxidation has been done by Stringer [13].

7. Application

The proposed model is applied to interpret the experimental results of steel D-9 (~13.6% Cr and ~13.6% Ni). The experiments were carried out in a LBE loop at temperature 550 °C [14]. The LBE flow velocity was 1.9 m/s and the oxygen level is in the range of 0.03–0.05 ppm. The weight changes and the oxide thickness were measured after 1000, 2000 and 3000 h exposures. For such experiments, no obvious erosion or oxide spallation is observed [14].

To obtain the parabolic oxidation rate constant and the mass transfer rate, the experimental results on weight changes are fitted using the early stage approximation (Eq. (19a)), shown in Fig. 6. The parabolic rate constant K_p and mass transfer rate K_r are 6.87×10^{-17} m^2/s and 7.04×10^{-13} m/s, respectively. The K_p value is about three times larger than that of SUS316 steel (2.64×10^{-17} m^2/s [15]) under the same oxygen partial pressure in gaseous environments. The difference may be attributed to the different Cr content in the two steels. Taking into account that there were many uncertain factors during the experiments [14], the present model captures the key features in the analysis of experimental results of steels in LBE environment and is suitable as a starting point to predict long-term behaviors.

Knowing K_p and K_r, the corresponding t_c and x_f are calculated as $t_c = 2.2$ yr and $x_f = 48.8$ μm. Because t_c is not the time to reach the steady state, it takes more than 2.2 yr to approach the limiting oxide thickness for the present cases. At the steady state, the substrate recession rate R is 3.4×10^{-13} m/s, leading to a corrosion rate 10.7 μm/yr that is consistent with the kinetic corrosion model results [12]. The above calculation indicates that the oxide layer can protect the steel and reduce the corrosion rate significantly if it is stable.

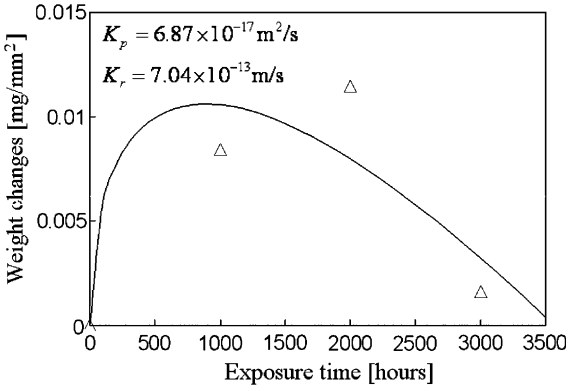

Fig. 6. Weight changes of steel D-9 in flowing LBE. Symbols are experimental results from Ref. [14], and the solid curve is the fitting results using Eq. (19a).

It should be noted that the present calculations only give very preliminary evaluation of the protective oxide behaviors of steels in flowing lead–alloy system. The microstructure and steel composition effects are neglected. Information on the protective oxide layer in liquid lead–alloy systems is still lacking and the existing experimental results are scattered. No general relation can be obtained yet, partly due to wide-ranging experimental conditions and materials, and partly due to a lack of consistent protocol to analyze and report all relevant results. For broad industrial applications, more theoretical and experimental studies should be carried in a more systematic framework.

8. Summary

High-temperature oxidation with scale removal is studied using the non-dimensional Tedmon's equation. The initial conditions are classified into distinct categories. The early stage and asymptotic (late stage) kinetics are discussed. Approximation equations, easily used for fitting experimental results, are derived. We show which simplified model is applicable in what range with what initial conditions. The proposed model is successfully applied to interpret the oxide behaviors of D-9 steel in flowing LBE. It is found for pre-oxidation cases:

1. If $X_0 < 1$, the non-dimensional thickness increases in time and approaches 1 from below. If $X_0 > 1$, the oxide thickness decreases in time and approaches 1 from above. If $X_0 = 1$, the thickness remains constant.
2. If $X_0 < f_O$ (oxygen mass fraction in the oxide), the specific weight change first increases, then decreases in time after reaching a peak. If $X_0 \geqslant f_O$, it decreases in time, and especially for $X_0 = 1$, the decrease is linear in time.
3. The asymptotic oxide thickness and the time constant are very sensitive to the rate of the linear scale removal, which can be used to control or adjust the desired oxide thickness. The asymptotic (long-term) substrate recession rate is determined by the linear scale removal rate and not by oxidation.
4. The present analysis provides clear guidance to using short-term experiments to predict long-term kinetics by extracting the relevant process parameters.

High-temperature oxidation is a very complicated process, especially for alloys, which involves multiple oxide layers and multi-component diffusion. More studies should be carried out theoretically and experimentally. Experiments on protective-scale removal through mass transfer corrosion in heavy liquid metal coolant (lead–bismuth and lead) systems are being performed at the Los Alamos National Laboratory for applications in advanced nuclear systems. For this specific application of using protective oxide to mitigate steel corrosion, more detailed analysis will be performed and reported separately. However, the general methodology outlined here should be applicable to a broad range of problems and applications.

Acknowledgements

The first and third authors acknowledge the support of Transmutation Research Program (TRP) at the University of Nevada, Las Vegas.

References

[1] C.S. Tedmon Jr., J. Electrochem. Soc. 113 (1966) 766.
[2] H. Taimatsu, J. Electrochem. Soc. 146 (1999) 3686.
[3] E.J. Opila, J. Am. Ceram. Soc. 86 (2003) 1238.
[4] Y.Y. Liu, Natesan, Surf. Coat. Technol. 36 (1988) 407.
[5] D.M. Rishel, F.S. Pettit, N. Birks, Mater. Sci. Eng. A 143 (1991) 197.
[6] V.A.C. Haanappel, T. Fransen, P.J. Gellings, High Temp. Mater. Process 10 (1992) 91.
[7] J.P. Tu, Corrosion 53 (1997) 365.
[8] F.H. Stott, C.Y. Shih, Mater. Corros. 51 (2000) 277.
[9] T.A. Ramanarayanan, S.N. Smith, Corrosion 41 (1990) 66.
[10] B.J. Downey, J.C. Bermeil, P.J. Zimmer, Corrosion 25 (1969) 502.
[11] M.J. Maloney, M.J. Mcnallan, Metall. Trans. B 16B (1985) 751.
[12] J. Zhang, N. Li, Report to Los Alamos National Laboratory, 2004, LA-UR-04-0869.
[13] J. Stringer, Oxid. Met. 5 (1972) 49.
[14] J. Zhang, N. Li, Y. Chen, A.E. Rusanov, J. Nucl. Mater. 336 (2004) 1.
[15] A.F. Smith, Corros. Sci. 22 (1982) 857.